Calculations on the current density and the voltage–current relation under a.c. conditions of filaments

R.A. Hartmann, D. Dijkstra*, F.P.H. van Beckum* and L.J.M. van de Klundert

University of Twente, Department of Applied Physics, PO Box 217, 7500 AE Enschede, The Netherlands
*University of Twente, Department of Applied Mathematics, PO Box 217, 7500 AE Enschede, The Netherlands

Received 8 April 1987; revised 8 April 1988

Technical applications of multifilamentary wires indicate that filaments are used in complex magnetic fields (a combination of non-parallel a.c./d.c. transverse and rotating fields) carrying an a.c./d.c. transport current of various frequency. Furthermore, due to technical manufacturing processes the filaments are heavily distorted. Therefore, a numerical model is developed to compute the current density of a filament of arbitrary shape in any external transverse field carrying an a.c./d.c. transport current. The great flexibility of the model is shown in several examples.

Keywords: superconducting cables; current distribution; mathematical models

Losses in superconducting cables can be divided into coupling loss, magnetization loss, and loss due to dynamic resistivity. For both the magnetization loss of the wires and the loss due to the dynamic resistivity, one has to know the exact current distribution inside the filaments. For the Carr[1] continuum model of a multifilamentary wire a voltage–current relation is needed. This relation is obtained from the current distribution of a filament. Therefore, we will consider the problem of determining the current distribution of filaments under several circumstances. Various numerical models have been developed to compute the current distribution of a type II superconducting cylindrical filament in a transverse applied field[2–6]. These methods are based on a parametrization of the boundary which separates the region of opposite saturation and non-saturated parts. A region, S, is defined to be saturated if $|j(r)| = j_c$, $r \in S$, and unsaturated if $|j(r)| = 0$. The problem of determining the current distribution in a filament carrying a time dependent transport current and placed in a time dependent transverse applied field is more difficult. The reason for this is that a priori the number of moving boundaries is not clear, and the number may change. A simple but robust numerical approach was first set up by Hartmann and Rem[7,8], which was developed to treat the problem of the number of moving boundaries. The method can compute the current distribution, magnetization, losses, etc., of a filament where the applied field can vary arbitrarily as a function of time and place. In addition to the problem of the number of moving boundaries we can also treat any shape of the cross-section of a filament and we can include the field dependence of j_c. The option of the shape of the filament is of interest because original circular filaments may be heavily distorted due to the manufacturing process. The numerical method is based on an algorithm predicting the current distribution and correcting it via an expression for the vector potential and the constitutive equations. An outline of the numerical approach will be given in the next section for uniform values of j_c. Field dependence of j_c can be included in this numerical set-up but is normally of no interest for fine filaments.

In the results section of this Paper we discuss three examples. We consider a circular filament in an a.c. transverse field with a d.c. transport current. Due to the transport current more moving boundaries will occur. We calculate the current density, the cross-sectional average value of the electric field along the axis of the filament and the magnetization. A circular filament in an angulary oscillating field with total angle variation $\pi/2$ is considered: the current density and the magnetization loss per cycle per unit volume are calculated. Finally, the magnetization losses due to a transverse applied field and an a.c. transport current of a circular and a square filament are compared.

In this Paper, the voltage–current relation is calculated for a square filament carrying an a.c. transport current placed in a d.c. transverse field; this is needed for the Carr approximation. To examine this result we derive a more accurate analytical expression for the voltage–

0011-2275/89/020101-08 $03.00

current relation which normally is used for loss calculation on multifilamentary wires[8]. Both results are compared.

Theory

Consider an infinitely long superconducting cylinder carrying a transport current, $I_A(t)$, in a transverse applied field, $\vec{B}_A(t)$. We assume that all electromagnetic fields are invariant with respect to translation along the z-axis, where the z-axis is chosen to be parallel to the axis of the superconductor. Therefore, we may describe the current density in a cross-section, S, of the cylinder by:

$$\vec{j} = j_z \vec{e}_z \tag{1}$$

It follows from Maxwell's equation and the Biot–Savart law that we may choose the following expression for the vector potential

$$\vec{A} = (A_x, A_y, A_z)$$

$$A_x(\vec{r}, t) = 0 \tag{2a}$$

$$A_y(\vec{r}, t) = 0 \tag{2b}$$

$$A_z(\vec{r}, t) = -\frac{\mu_0}{2\pi} \int_S j_z(\vec{r}', t) \ln|\vec{r} - \vec{r}'| \, dS(\vec{r}') - [\vec{r} \times \vec{B}_A(t)] \cdot \vec{e}_z + C(t) \tag{2c}$$

$\vec{r} = (x, y)$, $\vec{e}_z$ is the unit vector in the z direction, and where $C(t)$ is an arbitrary function of t. Thus, $\vec{B} = \nabla \times \vec{A}$ and $\nabla \times \vec{A} \to \vec{B}_A$ as $|\vec{r}| \to \infty$ if S is bounded.

From Maxwell's equation $\nabla \times \vec{E} = -\dot{\vec{B}}$ and $\nabla \times \dot{\vec{A}} = \dot{\vec{B}}$, thus it follows that

$$E_z \vec{e}_z = (-\partial_t A_z + \nabla . \Phi) \vec{e}_z \tag{3a}$$

where Φ is a scalar potential. One can easily see that Φ does not depend on $\vec{r}$ and consequently $\partial_z \Phi$ depends only on t, so we can choose $C(t)$ such that

$$E_z \vec{e}_z = -\partial_t A_z \vec{e}_z \tag{3b}$$

Equation (2c) is one relation between the scalar fields $j_z(\vec{r}, t)$ and $A_z(\vec{r}, t)$; the second relation is found in the constitutive equations: for all $\vec{r} \in S$

either

$$j_z = j_c(\vec{B}) \wedge E_z = -\partial_t A_z > 0$$

or

$$j_z = 0 \wedge E_z = -\partial_t A_z = 0 \tag{4a}$$

or

$$j_z = -j_c(\vec{B}) \wedge E_z = -\partial_t A_z < 0$$

where $j_c(\vec{B})$ is the critical current density.

The integration constant $C(t)$ in Equation (2) is determined by

$$\int_S j_z(\vec{r}, t) dS(\vec{r}) = I_A(t) \tag{4b}$$

In general, Equations (2c) and (4) cannot be solved analytically even for constant j_c and simple choices for the geometry. In the next section we will discuss a numerical method for constant j_c but arbitrary shape of S and any $\vec{B}_A(t)$, $I_A(t)$. In principle the current density for a non-constant j_c can be taken into account and treated in the same way as described in the next section.

Numerical model

We have considered Equations (2c) and (4), and developed a time-stepping iterative algorithm. First of all we discretize Equation (2c) by partitioning the cross-section S into a number of elements S_k such that S is the union of all S_k. These elements should be chosen so that the dimensions in both directions are approximately equal to obtain a good resolution. In every S_k we take a representation point, $\vec{r}_k$, as the centre of that element. We can discretize the integral (2c) for the vector-potential A_z at $\vec{r} = \vec{r}_k$ by

$$A_z(\vec{r}_k, t) = -\frac{\mu_0}{2\pi} \sum_m a_{km} j_m(t) - [\vec{r}_k \times \vec{B}_A(t)] \cdot \vec{e}_z + C(t)$$

with

$$a_{km} = \int_{S_m} \ln|\vec{r}_k - \vec{r}'| \, dS_m(\vec{r}')$$

$$j_m(t) = \frac{1}{\text{area } (S_m)} \int_{S_m} j_z(\vec{r}', t) dS_m(\vec{r}') \tag{5}$$

j_m is the total amount of current of element S_m. We define an element S_k to be saturated if

$$|j_k(t)| = j_c \tag{6}$$

and otherwise unsaturated.

Suppose that at time t_l there are $N_1(t_l)$ unsaturated elements and $N_2(t_l)$ saturated elements, such that $N_1(t_l) + N_2(t_l) = N$, the total number of elements; then for the next time-step we assume that this situation is a good prediction. Because of a change of the applied field or the transport current, however, there shall be a variation of the vector-potential, ΔA_z, and consequently the total current j_k of each element can be changed by Δj_k, say. To solve the N unknown Δj_k we need N equations. For each element, S_k, that is predicted to be unsaturated, we know that the vector-potential should be zero. This means that for all $N_1(t_l)$ unsaturated elements S_k, with centre $\vec{r}_k$, we have

$$\Delta A_z(\vec{r}_k) = A_z(\vec{r}_k, t_{l+1}) - A_z(\vec{r}_k, t_l) = -\frac{\mu_0}{2\pi} \sum_m a_{km} \Delta j_m + (\vec{r}_k \times \Delta \vec{B}_A) \cdot \vec{e}_z + \Delta C = 0 \tag{7}$$

However, we know that for each of the $N_2(t_l)$ saturated elements, if this situation was correct for $t_l + 1$, the total current must be equal to j_c

$$|j_k| = j_c$$

Equation (7) together with the equation for the total current

$$I_A(t_{l+1}) = \sum_k j_k(t_{l+1}) S_k \tag{8}$$

form a set of $N_1 + 1$ equations from which the N_1 unknown Δj_k and the unknown ΔC can be solved.

Of course we must check the solution to examine if the predicted situation was correct. Therefore, each unsaturated element at $t_l + 1$ must satisfy $|j_k| < j_c$ and

for each saturated element we must have sign $[\Delta A_z(\tilde{r}_k)] = -$ sign (j_k).

If an unsaturated or a saturated element does not satisfy the condition, we will change its type into saturated or unsaturated, respectively. In case of a constant j_c we only have to check those elements near to a moving boundary or a physical boundary, because in that particular situation new moving boundaries will always arise from a physical boundary.

Having determined the current density, one can easily calculate the mean value of E_z over the cross-section and the magnetization, as follows

$$\bar{E}_z(t) = \left[\sum_{k=1}^{N_2} \Delta A_z(\tilde{r}_k, t) S_k\right] S^{-1} \tag{9a}$$

$$M_x(t) = \sum_{k=1}^{N} j_k(t) S_k y_k \tag{9b}$$

$$M_y(t) = -\sum_{k=1}^{N} j_k(t) S_k x_k \qquad \text{with } (x_k, y_k) = \tilde{r}_k \tag{9c}$$

Results

In this section we discuss three examples of filaments placed in an arbitrary applied field. The first example is of a circular filament in an unidirectional a.c. applied field carrying a d.c. transport current. This is an example where more than one moving boundary is expected. The new boundaries, however, as mentioned before, will always arise from a physical boundary. *Figures 1a* and *b* show the time dependence of the applied field and the transport current. The maximum value of the applied field is equal to the penetration field $B_p = 2\mu_0 j_c R/\pi$. That means that for this value of the applied field, without transport current, the filament is completely saturated. By adding a transport current complete saturation will occur for smaller values of the applied field. *Figure 2* shows the current distribution, where the sign denotes whether the current flows in the z or $-z$ direction. The numbers on the figures correspond to those of *Figure 1a*, the time dependence of the applied field. In addition to the current distribution we have also calculated the mean value of E_z over the cross-section and the magnetization parallel to the applied field as function of time. A first order approximation of the mean value of E_z under the condition that the time derivative of the applied field is small, can be given by

$$\bar{E}_z = -d_t B_A R\, I_A/(2\, I_c)$$

Although we have achieved this expression for a square filament, we can use it for a circular filament (discussed below). The results are given in *Figures 1c* and *d*.

The second example is that of a circular filament in a angulary oscillating transverse applied field where $|B_A|$ is constant. *Figure 3* shows the sign of the current densities as a function of time for $|B_A| = 2B_p$ and $|B_A| = 6B_p$, respectively, where B_p is the penetration field. The applied field is oscillating with total angle variation $\pi/2$. The arrow in the figures denotes the direction of the applied field. Although, for high fields, the original shape of the moving interface is very quickly restored, the magnetization loss per cycle per unit volume will be much smaller than that of a purely rotating field. In the latter case the moving boundary is of constant shape and rotates with the angular velocity of the applied field, so the magnetization is constant[4,5].

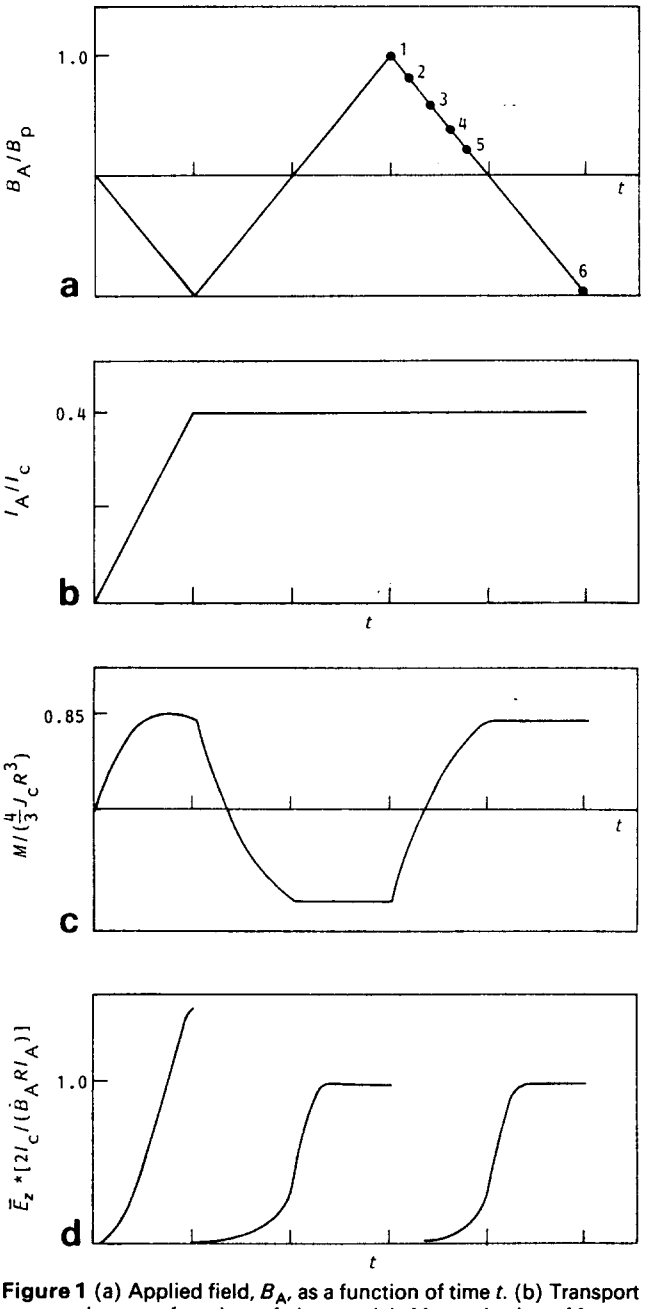

Figure 1 (a) Applied field, B_A, as a function of time t. (b) Transport current, I_A, as a function of time, t. (c) Magnetization, M, as a function of t corresponding to *Figure 1a*. (d) Cross-sectional averaged value of the electric field, $\bar{E}_z$, along the axis of the filament as a function of t corresponding to *Figure 1a*

The oscillating field, however, causes a smaller magnetization loss per cycle because the original shape of the moving boundary is heavily distorted for some time. Therefore, we examine whether the rotating or the alternating component of the applied field is responsible for the magnetization loss.

In *Figure 4* we have computed the loss per cycle per unit volume due to the magnetization of a circular filament as a function of the applied field for three comparable situations. The first situation (see the solid line in *Figure 4*) describes a filament in an oscillating transverse applied field with total angle $\pi/2$. The loss was computed with our numerical method using the following

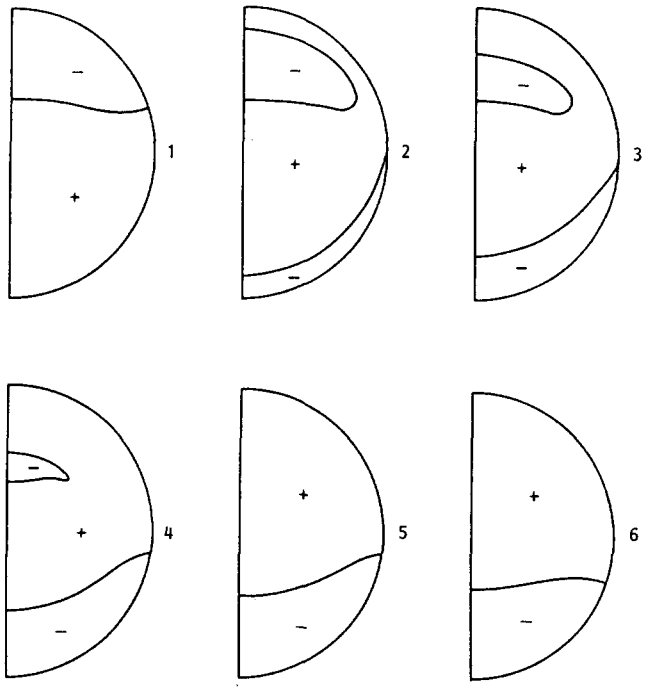

Figure 2 Current distribution in a circular filament placed in an external a.c. magnetic field, $B_A(t)$, carrying a d.c. transport current, $I_A(t)$. Numbers 1–6 refer to the points of time given in *Figure 1a*

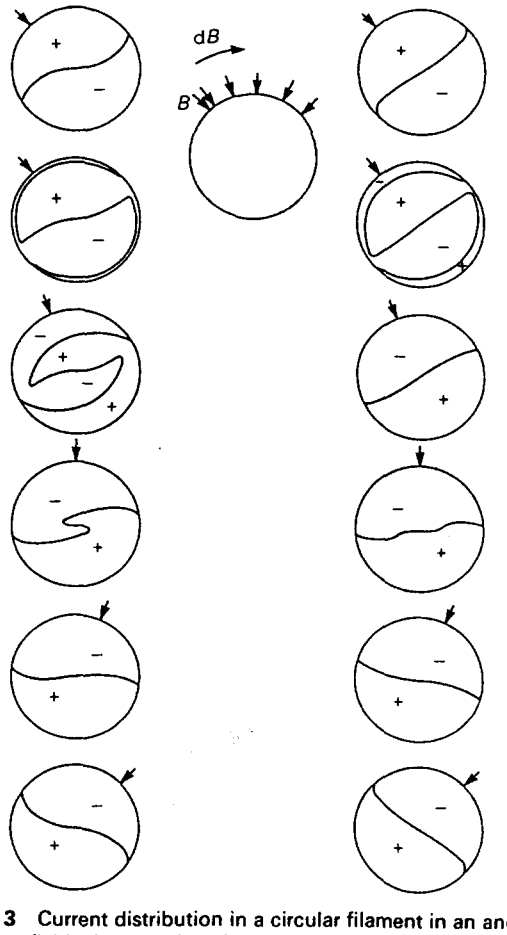

Figure 3 Current distribution in a circular filament in an angulary oscillating field with a total angle variation of $\pi/2$, without transport current. The figures at the left-hand side are calculated for $|B_A| = 2B_p$ and the right-hand side for $|B_A| = 6B_p$. The arrows denote the directions of the applied field

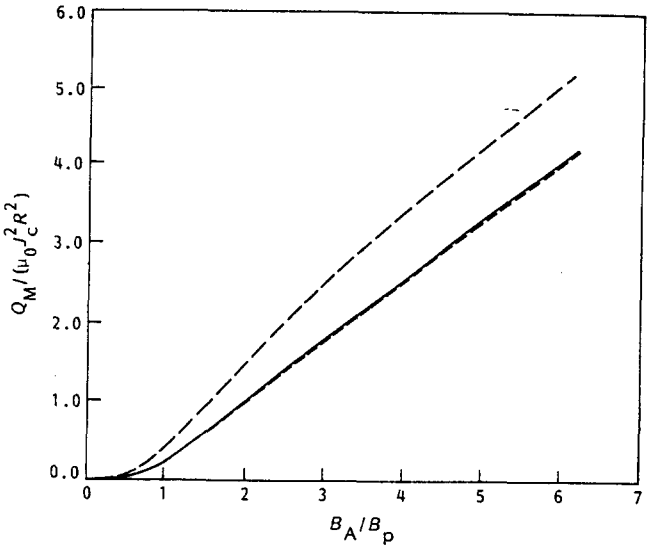

Figure 4 Magnetization loss, Q_M, per cycle per unit volume of a circular filament for three different situations. – – – –, Calculated using the expression of Pang[4,5] for a circular filament in a rotating field; – – – – – – – – – –, calculated using the expression of Zenkevitch[9] for a circular filament in an a.c. transverse field; ———, calculated using the numerical method outlined in this Paper for a circular filament in an angulary oscillating transverse field rotating with total angle of $\pi/2$. All three curves are given as functions of the applied field amplitude

expression

$$Q_M = \frac{2}{\pi R^2} \int_{-\pi/4}^{\pi/4} M_\perp |B_A| \, d\phi \tag{10}$$

with $M_\perp$ the component of the magnetization perpendicular to the applied field.

The upper dashed line in *Figure 4* is the loss per half cycle per unit volume of a filament in a rotating field for the stationary situation. This loss was calculated using an expression developed by Pang[4,5]

$$Q_M = \frac{4\pi}{3\mu_0} |B_A| B_p [1 - \exp(-4\beta^2) - 8\beta^3 \exp(-4.75\beta)] \tag{11}$$

$$\beta = \frac{|B_A|}{\mu_0 j_c R}$$

where B_p is the penetration field, R is the radius, and j_c is the critical current density.

The lower dashed line in *Figure 4*, which is very close to the solid one, is the loss per cycle per unit volume of a filament in an a.c. transverse field with amplitude $\hat{B}_A = (2^{\frac{1}{2}}|B_A|)/2$. An expression for the loss per cycle per unit volume was first given by Zenkevitch[9]

$$\begin{aligned} Q_M &= \frac{8}{3\mu_0}\frac{\hat{B}_A^3}{B_p} - \frac{4}{3\mu_0}\frac{\hat{B}_A^4}{B_p^2} \qquad \text{if } \hat{B}_A \leqslant B_p \\ &= \frac{8}{3\mu_0}\hat{B}_A B_p - \frac{4}{3\mu_0} B_p^2 \qquad \text{if } \hat{B}_A > B_p \end{aligned} \tag{12}$$

Figure 4 shows that the loss of a filament in an angulary oscillating field with a total angle $\pi/2$, perfectly coincides with the loss of a filament in a comparable a.c. transverse field of appropriately chosen amplitude. Therefore, we may conclude that the loss of a filament in an oscillating applied field, or a combination of a rotating and an a.c. transverse applied field, is comparable with the loss of a filament in a purely a.c. transverse field.

As mentioned earlier, the numerical method described can treat any shape of cylindrical filament. In the last example, we compare the magnetization loss of a circular and square filament. The filaments are placed in a transverse magnetic field, carrying an a.c. transport current. *Figure 5* shows the scaled magnetization loss per cycle per unit volume of a circular and square filament, where the applied field is perpendicular to one of the sides of the square filament. Here the scaled magnetization loss was defined by

$$Q_m^* = Q_m/(|\vec{M}_p|B_p) \tag{13a}$$

$$Q_m = \oint \vec{M} \cdot d\vec{B}_A \tag{13b}$$

where $\vec{M}_p$ is the magnetization if $|B_A| = B_p$, and B_p is the penetration field.

The scaling factors can be found easily: for a circular filament $|\vec{M}_p|$ and B_p

$$|\vec{M}_p| = \frac{4}{3} j_c R^3$$

$$B_p = \frac{2}{\pi} \mu_o j_c R \tag{14a}$$

and for a square filament

$$|\vec{M}_p| = \frac{1}{4} j_c d^3$$

$$B_p = \frac{(2\ln 2 + \pi)}{4\pi} \mu_o j_c d \tag{14b}$$

We can see that the scaled magnetization loss of a circular filament coincides perfectly with that of a square filament. From this result we may expect that for filaments with arbitrary cross-section, the magnetization loss per cycle per unit volume will behave identically but for a geometrical factor only. This factor can be described by

$$f = \frac{|\vec{M}_{p,1}|B_{p,1}}{|\vec{M}_{p,2}|B_{p,2}} \tag{15}$$

such that $Q_{m,1} = fQ_{m,2}$

For example, if we have a circular and a square filament with cross-sections of equal area, the geometric factor can be achieved by

circle area $= \pi R^2$

square area $= d^2$

resulting in $d = \pi^{\frac{1}{2}} R$

and using Equation (13)

$$f = \frac{3\pi^2(2\ln 2 + \pi)}{128} \approx 1.047 \tag{16}$$

with Q_m (square) $= fQ_m$(circle). This means that the magnetization loss per cycle per unit volume of a square filament is approximately 5% more than the loss of a circular filament with equal cross-sectional area.

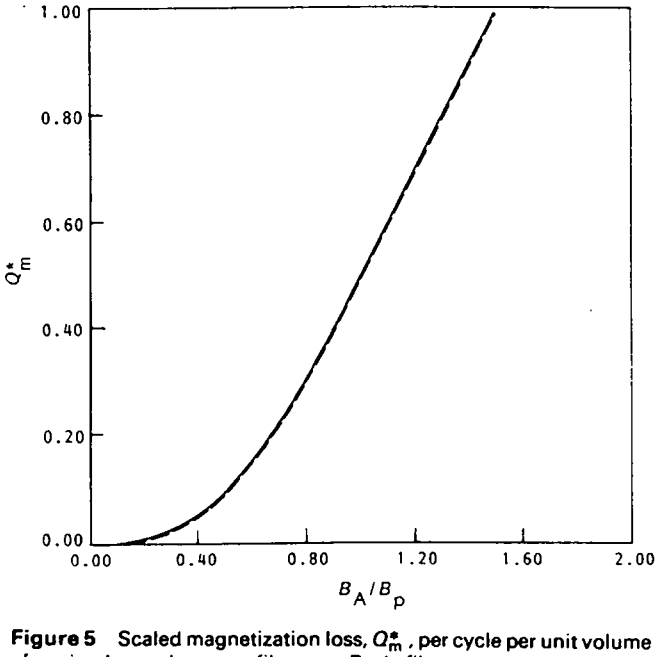

Figure 5 Scaled magnetization loss, Q_m^*, per cycle per unit volume of a circular and square filament. Both filaments are placed in a transverse field carrying an a.c. transport current. ———, Circular filament; – – –, square filament. For scaling factors see text Equations (14a) and (14b)

Dynamic resistivity of a filament

Calculation of the loss due to the dynamic resistivity of filaments of multifilamentary wires requires an accurate voltage–current relation of the filaments. Loss calculations on cables and wires consisting of large filaments especially need such an expression. We develop an analytical expression for the voltage–current relation of a square filament below. As seen in the third example given in the previous section, the difference between a circular and a square filament is very small. Therefore, we may in the future use the expression for calculations on circular filaments. We have also verified the expression by comparing it with numerical results. The latter are obtained using our numerical method for a filament with a square cross-section.

Voltage–current relations of filaments

We consider a square filament in an applied transverse field $\tilde{\vec{B}}_A(t) = \tilde{B}_A(t)\hat{e}_x$ carrying an a.c. transport current $\tilde{I}_A(t)$. Instead of using the physical electromagnetic fields $\tilde{\vec{B}}, \tilde{\vec{j}}, \tilde{\vec{E}}, \tilde{\vec{A}}$ and $\tilde{I}^A$ we define dimensionless fields by

$$\hat{B} = \frac{\tilde{\vec{B}}}{\mu_0 \tilde{j}_c d}$$

$$\hat{j} = \frac{\tilde{\vec{j}}}{\tilde{j}_c}$$

$$\hat{E} = \frac{\tilde{\vec{E}}}{\mu_0 \tilde{j}_c d^2} \tag{17}$$

$$\hat{A} = \frac{\tilde{\vec{A}}}{\mu_o \tilde{j}_c d^2}$$

$$I_A = \frac{\tilde{I}_A}{\tilde{I}_c}$$

and space is scaled by d, the side of the filament

$$x = \frac{\tilde{x}}{d}$$

$$y = \frac{\tilde{y}}{d}$$

Using these definitions, Maxwell's equations and the constitutive equations now read

$$\nabla \times \vec{B} = j_z \vec{e}_z \tag{18a}$$

$$\nabla \times \vec{E} = -\dot{\vec{B}}_A - \dot{\vec{B}}_I \tag{18b}$$

$$j_z = \begin{cases} +1 & \text{if } E_z < 0 \\ 0 & \text{if } E_z = 0 \\ -1 & \text{if } E_z > 0 \end{cases} \tag{18c}$$

where we have assumed that all electromagnetic fields are invariant with respect to translation along the z axis, where the z axis is chosen to be parallel to the axis of the conductor.

The first and classical analytical approach is to neglect the induced field, $\vec{B}_I$. Using this assumption we can solve Maxwell's equations easily

$$\partial_y E_z = -\dot{B}_A \geqslant E_z = -\dot{B}_A y + E_0 \tag{19a}$$

and E_0 is defined by

$$j_z = \begin{cases} +1 & E_z < 0 \quad y > y_0 \\ 0 & E_z = 0 \quad y = y_0 = \dfrac{E_0}{\dot{B}_A} \\ -1 & E_z > 0 \quad y < y_0 \end{cases} \tag{19b}$$

This gives us $E_0 = \dot{B}_A y_0$ where the boundary $y = y_0$ separates the regions of different saturation (see *Figure 6*). This means that

$$y_0 = \frac{I_A}{2}$$

where I_A is the transport current.

It follows immediately from Equation (19a) that we can describe $\bar{E}_z$, the mean value of E_z over the cross-section, by

$$\bar{E}_z = \dot{B}_A I_A / 2 \tag{20}$$

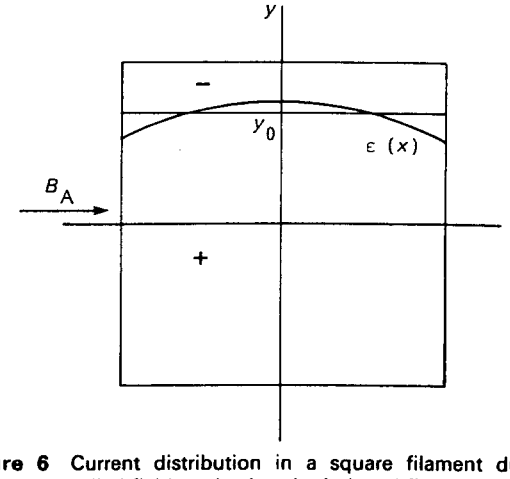

Figure 6 Current distribution in a square filament due to a transverse applied field neglecting the induced field, the boundary is given by y_0. The boundary $\varepsilon(x)$ denotes a first-order approximation of the current distribution if the induced field is not neglected

To achieve a more accurate approximation for the voltage-current relation we consider a small disturbance Δj_z of the current density at $y = y_0$. Instead of calculating the induced field $\vec{B}_I$ due to the disturbance, we will compute the vector-potential A_z as a function of Δj_z at $y = y_0$ by the Biot–Savart law. Taking the expression for A_z into account we can solve Maxwell's equation $\nabla \times \vec{E} = -\dot{\vec{B}}$, deriving a new expression for $\bar{E}_z$ as a function of i, the total current.

Defining the vector-potential $\vec{A}$ by $\nabla \times \vec{A} = \vec{B}$ and $\nabla \cdot \vec{A} = 0$, the first Maxwell's equation $\nabla \times \vec{B} = \mu_0 \vec{j}$ now reads

$$\Delta_L A_z = -j_z \tag{21}$$

where Δ_L is the Laplace operator. The disturbance Δj_z is given by

$$\Delta j_z = \begin{cases} 2\delta(y - y_0)\partial_t y_0 & -\frac{1}{2} \leqslant x \leqslant \frac{1}{2} \\ 0 & \text{elsewhere} \end{cases} \tag{22}$$

so we can describe the variation $\Delta(\Delta_L A_z)$ as

$$\Delta(\Delta_L A_z) = -2\delta(y - y_0)\partial_t y_0 \quad -\tfrac{1}{2} \leqslant x \leqslant \tfrac{1}{2} \tag{23}$$

and $\dot{A}_z$ by the Biot–Savart law as

$$\dot{A}_z(x, y) = -\frac{1}{4\pi} \int_{x'} \int_{y'} \Delta j_z \ln[(x' - x)^2 + (y' - y)^2] dx' dy' + E_0' \tag{24}$$

$$= -\frac{1}{2\pi} \partial_t y_0 \Big[(x' - x)\ln[(x' - x)^2 + (y_0 - y)^2] - 2x' + 2(y_0 - y)\arctan\left(\frac{x' - x}{y - y_0}\right) \Big] \Big|_{x' = -\frac{1}{2}}^{\frac{1}{2}} + E_0'$$

Now we can solve for E_z, using the second Maxwell's equation

$$(\nabla \times \vec{E}) = -\dot{\vec{B}}_A - \dot{\vec{B}}_I = \nabla \times [(-\dot{B}_A y + E_0)\vec{e}_z - \dot{A}_z \vec{e}_z] \tag{25}$$

$$E_x = E_y = 0$$

This results in

$$E_z = -\dot{B}_A y + E_0 - \dot{A}_z$$

from which we obtain

$$\bar{E}_z = E_0 - \bar{\dot{A}}_z \tag{26}$$

where $\bar{\dot{A}}_z$ is the average of $\dot{A}_z$ over the cross-section of the filament

$$\bar{\dot{A}}_z = -\frac{1}{2\pi} \partial_t y_0 \int_{x = -\frac{1}{2}}^{\frac{1}{2}} \int_{y = -\frac{1}{2}}^{\frac{1}{2}} \Big\{ (x' - x)\ln[(x' - x)^2 + (y - y_0)^2] - 2x' + 2(y_0 - y)\arctan\left(\frac{x' - x}{y_0 - y}\right) \Big\} \Big|_{x' = -\frac{1}{2}}^{\frac{1}{2}} dy dx + E_0'$$

$$= -\frac{1}{48\pi} \partial_t y_0 \Big\{ 16\pi - 88 - 48\ln(2) + (-4 - 24i + 12i^2)\arctan\left(\frac{2}{1 - i}\right) + (-4 + 24i + 12i)\arctan\left(\frac{2}{1 + i}\right) + 2(1 - i)^3 \ln(1 - i)$$

$$+2(1+i)^3\ln(1+i)$$
$$+(11-9i+3i^2+i^3)\ln[4+(1-i)^2]$$
$$+(11+9i-3i^2+i^3)\ln[4+(1+i)^2]\Big\}+E'_0 \qquad (27)$$

with i the total current.

To calculate the constant E'_0 we have first to compute the new interface, $y'_0(x)$, using the constitutive equations. Once the current distribution is determined we will require that the total amount of current, i, is equal to the applied current, $I_A(t)$. This leads to an equation for E'_0.

At the new boundary $y'_0(x) = y_0(x) + \varepsilon(x)$ we can describe $E_z(x, y)$ as

$$\begin{aligned}E_z[y'_0(x)] &= E_z[y_0+\varepsilon(x)]\\ &= -[y_0+\varepsilon(x)]\dot{B}_A + E_0 - \dot{A}_z[x, y_0+\varepsilon(x)]\\ &= -\dot{B}_A y_0 + E_0 - \dot{A}_z(x, y_0) - \dot{B}_A\varepsilon(x) + O[\varepsilon^2(x)]\end{aligned} \qquad (28)$$

Since the new boundary $y'_0(x)$ separates the regions of different saturation, we know that at $y'_0(x)$, $E[y'_0(x)]$ is zero

$$\begin{aligned}E_z[y'_0(x)] &= -\dot{B}_A y_0 + E_0 - \dot{A}_z(x, y_0) - \dot{B}_A\varepsilon(x)\\ &= -\dot{A}_z(x, y_0) - \dot{B}_A\varepsilon(x) = 0\end{aligned} \qquad (29)$$

This gives us an expression for $\varepsilon(x)$ and hence $y'_0(x)$

$$\varepsilon(x) = -\dot{A}_z(x, y_0)/\dot{B}_A$$
$$y'_0(x) = y_0 + \varepsilon(x) = y_0 - \dot{A}_z(x, y_0)/\dot{B}_A \qquad (30)$$

with

$$\dot{A}_z(x, y_0) = -\frac{1}{\pi}\partial_t y_0[(\tfrac{1}{2}-x)\ln(\tfrac{1}{2}-x) + (\tfrac{1}{2}+x)\ln(\tfrac{1}{2}+x) - 1] + E'_0$$

Figure 6 shows $\varepsilon(x)$ in the case where Δj_z is positive (for Δj_z negative $\varepsilon(x)$ changes sign).

Now that the boundary $y'_0(x)$ is known, we can calculate the total current

$$\begin{aligned}i &= I_A + 2\int_{x=-\frac{1}{2}}^{\frac{1}{2}}\varepsilon(x)\mathrm{d}x\\ &= I_A - \frac{2}{\dot{B}_A}\int_{x=-\frac{1}{2}}^{\frac{1}{2}}\dot{A}_z(x, y_0)\mathrm{d}x\\ &= I_A - \frac{2}{\dot{B}_A}\left(\frac{\partial_t y_0}{2\pi} + E'_0\right)\end{aligned} \qquad (31)$$

If we require the total current, i, to be equal to the applied current, I_A, we find for E'_0

$$E'_0 = -\frac{\partial_t y_0}{2\pi} \qquad (32)$$

Substituting this expression for E'_0 in Equation (26), we get for $\bar{E}_z$

$$\bar{E}_z = E_0 + \partial_t y_0 f(i)$$

with

$$f(i) = \frac{1}{48\pi}\Big\{16\pi - 64 - 48\ln(2) + (-4-24i+12i^2)\arctan\left(\frac{2}{1-i}\right) + (-4+24i+12i^2)\arctan\left(\frac{2}{1+i}\right) + 2(1-i)^3\ln(1-i) + 2(1+i)^3\ln(1+i) + (11-9i+3i^2+i^3)\ln[4+(1-i)^2] + (11+9i-3i^2+i^3)\ln[4+(1+i)^2]\Big\} \qquad (33)$$

$$E_0 = y_0\dot{B}_A$$
$$y_0 = \frac{i}{2}$$
$$i = I_A$$

and

$$\partial_t y_0 = \frac{1}{2}\partial_t i$$

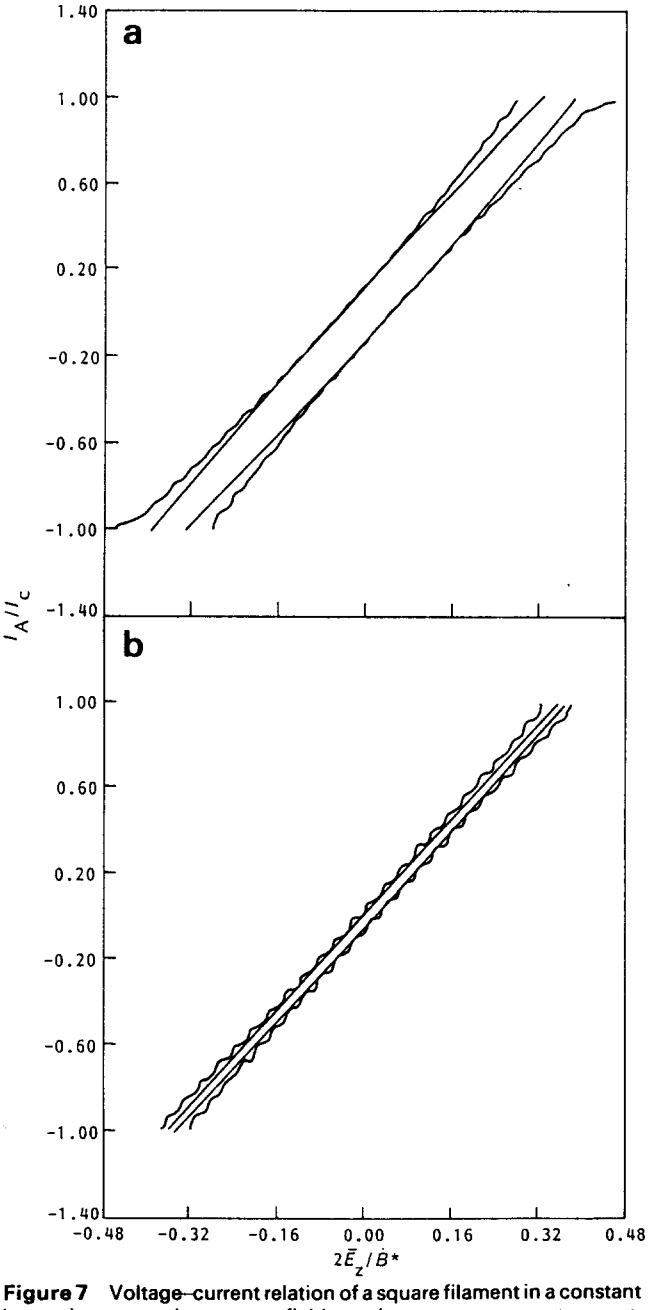

Figure 7 Voltage–current relation of a square filament in a constant increasing external transverse field carrying an a.c. transport current. ~~~~, Calculated using the numerical method outlined in this Paper; ———, calculated using the analytical expression developed for the voltage–current relation. (a) $n = 3$; (b) $n = 12$

Results

In the previous section we have derived an expression for the voltage–current relation of a square filament. The approximation becomes better for a small ratio $(\partial I_A/\partial t)/(\partial B_A/\partial t)$ because the hysteresis loss is small. Therefore, we will describe Equation (33) as

$$\frac{2\bar{E}_z}{\dot{B}_*} = \left[I_A B_p + \frac{1}{n} f(I_A) \right] \tag{34}$$

where

$$\dot{B}_A = B_p \dot{B}_*$$

and

$$\frac{1}{n} = \frac{(\partial I_A/\partial t)}{(\partial B_*/\partial t)}$$

To compare this expression with our numerical model, we have calculated the voltage–current relation for the situations $n = 3$ and $n = 12$ (see *Figure 7a* and *b*).

For large n the hysteresis loss becomes zero and in that case the voltage–current relation can be described by

$$\frac{2\bar{E}_z}{\dot{B}^*} = I_A B_p$$

with

$$B_p = \left(\ln 2 + \frac{\pi}{2} \right) \Big/ (2\pi)$$

the penetration field of a square filament.

Both examples show that the results have a perfect agreement for small values of $|I_A|$. The deviations near $|I_A| = 1$ are caused by the fact that we assumed $\varepsilon(x)$ to be independent of y_0, which is incorrect if y_0 is near one of the sides of the filament. Secondly one can see that the numerical results show an oscillating behaviour. This is caused by the grid which discretizes the continuous voltage–current relation. This means that a small change in the applied field or in the transport current does not change the number of saturated and unsaturated regions, and hence $\bar{E}_z$ will not change.

Conclusion

In this Paper we have presented a numerical method for calculating the current distribution of filaments. The filaments may have an arbitrary shape of cross-section and can be placed in any applied magnetic field of any behaviour predescribed in place and time. Furthermore, the filaments may carry an arbitrary transport current.

As we have shown in the examples, the described method can be used to treat complicated problems of calculating current distributions in a general way. The method can also handle the problem of a number of simultaneously moving boundaries and the field and position dependence of the critical current density can be incorporated. Therefore, we may conclude that we have succeeded in developing a robust algorithm for calculating the current density, magnetization and dynamic resistivity of superconducting filaments.

References

1 **Carr Jr, W.J.** *J Appl Phys* (1974) **45** 929
2 **Minervini, J.V.** Analysis of loss mechanism in superconducting windings of rotating electric generators *PhD Thesis* MIT, USA (1981)
3 **Kato, Y., Hanawaka, M. and Yamafuji, K.** *Jpn J Appl Phys* (1976) **15** 695
4 **Pang, C.Y., McLaren, P.G. and Campbell, A.M.** *Proc ICEC 8* Butterworths, Guildford, UK (1980) 739
5 **Pang, C.Y., McLaren, P.G. and Campbell, A.M.** *IEEE Trans Magn* (1981) 134
6 **Ashkin, M.** *J Appl Phys* (1979) **50** 8060
7 **Hartmann, R.A., Rem, P.C. and van de Klundert, L.J.M.** *Proc ICEC 11* Butterworths, Guildford, UK (1986) 781
8 **Rem, P.C.** Numerical models for a.c. superconductors *PhD Thesis* University of Twente, The Netherlands (1986)
9 **Zenkevitch, V.B., Zheltov, V.V. and Romanyuk, A.S.** *Dokl Acad Nauk USSR* (1980) **251** 339